BIOCHEMISTRY
including biophysical chemistry & molecular biology

Article

pubs.acs.org/biochemistry

Mechanistic Characterization of a 2-Thioxanthine Myeloperoxidase Inhibitor and Selectivity Assessment Utilizing Click Chemistry–Activity-Based Protein Profiling

Jessica Ward,[†] Samantha N. Spath,[†] Brandon Pabst,[†] Philip A. Carpino,[‡] Roger B. Ruggeri,[‡] Gang Xing,[†] Anna E. Speers,[§] Benjamin F. Cravatt,[§] and Kay Ahn*[,†]

[†]Cardiovascular and Metabolic Diseases Research Unit and [‡]Medicinal Chemistry, Pfizer Worldwide Research and Development, Cambridge, Massachusetts 02139, United States

[§]The Skaggs Institute for Chemical Biology and Department of Chemical Physiology, The Scripps Research Institute, La Jolla, California 92037, United States

Supporting Information

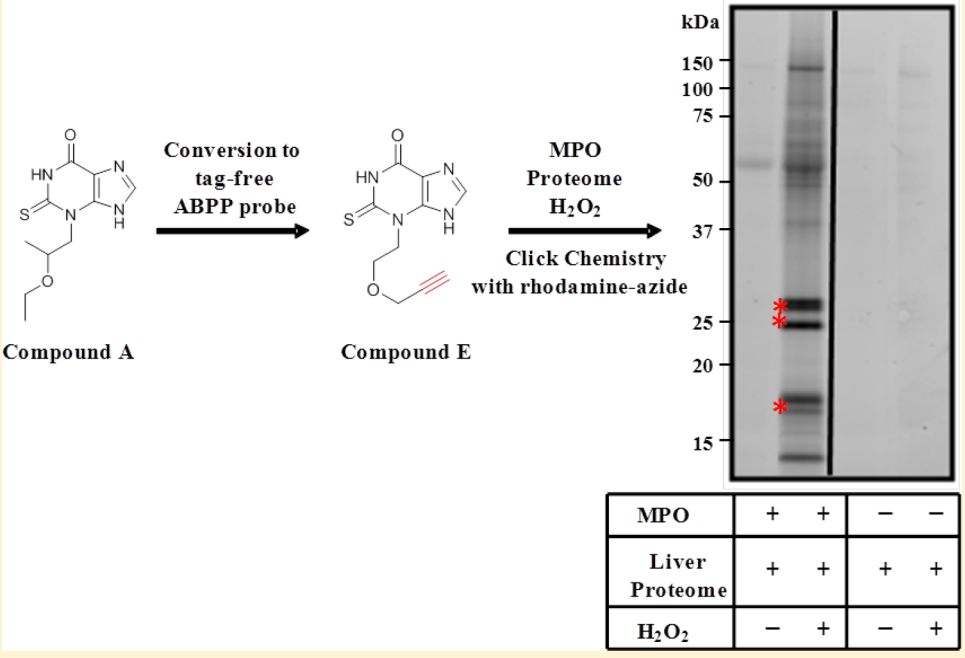

ABSTRACT: Myeloperoxidase (MPO) is a heme peroxidase that catalyzes the production of hypochlorous acid. Despite a high level of interest in MPO as a therapeutic target, there have been limited reports about MPO inhibitors that are suitable for evaluating MPO in pharmacological studies. 2-Thioxanthine, 3-(2-ethoxypropyl)-2-thioxo-2,3-dihydro-1*H*-purin-6(9*H*)-one (**A**), has recently been reported to inhibit MPO by covalently modifying the heme prosthetic group. Here we report a detailed mechanistic characterization demonstrating that **A** possesses all the distinguishing features of a mechanism-based inactivator. **A** is a time-dependent MPO inhibitor and displays saturable inactivation kinetics consistent with a two-step mechanism of inactivation and a potency (k_{inact}/K_I ratio) of 8450 ± 780 M^{-1} s^{-1}. MPO inactivation by **A** is dependent on MPO catalysis and is protected by substrate. **A** reduces MPO compound I to compound II with a second-order rate constant of (0.801 ± 0.056) × 10^6 M^{-1} s^{-1}, and its irreversible inactivation of MPO occurs prior to release of the activated inhibitory species. Despite its relatively high selectivity against a broad panel of more than 100 individual targets, including enzymes, receptors, transporters, and ion channels, we demonstrate that **A** labels multiple other protein targets in the presence of MPO. By synthesizing an alkyne analogue of **A** and utilizing click chemistry–activity-based protein profiling, we present that the MPO-activated inhibitory species can diffuse away to covalently modify other proteins, as reflected by the relatively high partition ratio of **A**, which we determined to be 15.6. This study highlights critical methods that can guide the discovery and development of next-generation MPO inhibitors.

Received: October 1, 2013
Revised: November 20, 2013
Published: November 20, 2013

Myeloperoxidase (MPO, EC 1.11.1.7) is a member of the heme peroxidase family of enzymes and catalyzes the synthesis of hypochlorous acid (HOCl) in the presence of hydrogen peroxide (H_2O_2) and chloride ion (Cl^-). MPO is stored in the granules of neutrophils and monocytes, with estimates varying from 1 to 2% of the dry weight of the cells to more than 5% of total cellular proteins, and is released upon leukocyte activation. MPO activity is important for the normal host defense mechanism as it is released into phagosomes that contain the endocytosed pathogens. However, under pathological conditions, persistent activation of the MPO–H_2O_2 system can initiate chlorination, nitration, and oxidative cross-linking of lipids, DNA, and proteins.[1,2] Therefore, MPO is implicated in the pathogenesis of many disorders such as neuroinflammation, Parkinson's disease, atherosclerosis, cardiovascular disease, and rheumatoid arthritis.[3−7]

Mature MPO is a 146 kDa dimer with a single disulfide bridge between symmetry-related halves (73 kDa), each of which contains two polypeptides of 14.5 and 58.5 kDa, the latter being N-glycosylated at multiple sites. Its active site is built around a heme prosthetic group with a distinctive three-point attachment to the polypeptide. Its protoporphyrin IX-based heme group is attached to the polypeptide chains through ester linkages with the carboxylic acid groups of Asp260, Glu408, and a sulfonium bond between the 2-vinyl group of heme and the sulfur atom of Met409.[8−11] MPO is closely related to the other mammalian peroxidases, eosinophil peroxidase, lactoperoxidase, and thyroid peroxidase, which share a similar protein structure.[12]

MPO possesses both halogenation (chlorination) and peroxidation activity and undergoes multiple redox reactions throughout the catalytic cycle. The halogenation reaction involves the native ferric enzyme [Fe(III) Por] undergoing a two-electron oxidation reaction with H_2O_2 producing the highly reactive compound I [Fe(IV)=O $Por^{\bullet+}$] form of the enzyme (reaction I). Through a two-electron reduction reaction, compound I reacts with chloride (or other halides) and is reduced back to the native enzyme generating HOCl [or HOX (reaction II)].[13] Alternatively, in the peroxidation cycle, compound I is able to react with various organic substrates (AH_2) via a one-electron reduction reaction generating the compound II [Fe(IV)=O Por] form of the enzyme (reaction III). An additional one-electron reduction reaction of compound II by the organic substrate regenerates native MPO (reaction IV).[12] Additional redox intermediates of MPO exist, including the ferrous enzyme [Fe(II) Por] and compound III [Fe(III)-$O_2^{\bullet-}$ Por]; however, these do not participate in the normal halogenation or peroxidase cycles.[1,2]

$$\text{MPO} + H_2O_2 \rightarrow \text{compound I} + H_2O \quad \text{(I)}$$

$$\text{compound I} + Cl^- + H^+ \rightarrow \text{MPO} + \text{HOCl} \quad \text{(II)}$$

$$\text{compound I} + AH_2 \rightarrow \text{compound II} + {}^{\bullet}AH \quad \text{(III)}$$

$$\text{compound II} + AH_2 + H^+ \rightarrow \text{MPO} + {}^{\bullet}AH + H_2O \quad \text{(IV)}$$

Despite extensive implication of MPO in various diseases and a high level of interest in MPO as a therapeutic target, the literature about promising MPO inhibitors is sparse. Additionally, only a few compounds were investigated in detail to clarify the molecular mechanism of MPO inactivation. The 2-thioxanthine derivatives were reported to be mechanism-based inactivators of MPO that modify the heme prosthetic groups of the enzyme.[14,15] By utilizing multistage mass spectrometry combined with crystallographic analysis, we recently reported that the 2-thioxanthine analogue represented by 3-(2-ethoxypropyl)-2-thioxo-2,3-dihydro-1*H*-purin-6(9*H*)-one [**A** (Figure 1A)] inhibits MPO by forming a covalent linkage between the methyl substituent of the heme pyrrole D ring of the MPO heme and the sulfur atom of **A**.[15]

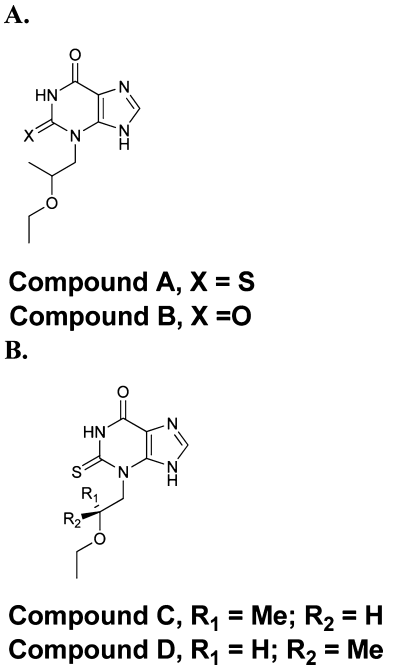

Figure 1. Compound structures. (A) Compound **A** and compound **B**, the xanthine analogue of compound **A**. (B) Compound **C** and compound **D**, the two stereoisomers of compound **A**.

To assess whether **A** would serve as a useful pharmacological tool in studying the effect of MPO inhibition, we have characterized **A** in detail, including its mechanism of inhibition, inhibition kinetics, and extensive selectivity assessment. In this report, we describe a detailed mechanistic study for MPO inhibition by assessing **A** with respect to all distinguishing features of a mechanism-based inactivator. To be an effective mechanism-based inactivator, it is important to possess a high inactivation efficiency, which is measured by the partition ratio. On the basis of the relatively high partition ratio of **A** we determined, indicating that the activated inhibitory species of **A** generated by MPO is released into solution and can label other proteins, we assessed the selectivity of **A** against proteomes as well as against a broad spectrum of more than 100 individual targets. To assess whether **A** could modify other protein targets in proteomes derived from human and mouse sources, we synthesized an alkyne analogue of **A** and utilized click chemistry–activity-based protein profiling (CC–ABPP). Here we provide evidence that **A** is completely unreactive in labeling proteins in liver proteomes. However, **A** can covalently modify multiple other protein targets in liver proteomes when MPO is present.

This study demonstrates that **A** could potentially serve as a valuable pharmacological tool for studying MPO. Importantly, the results and analytical strategies described in this report should facilitate further development of MPO inhibitors with greater inactivation efficiency and prevent the formation of covalent adducts with other protein targets.

dx.doi.org/10.1021/bi401354d | *Biochemistry* 2013, 52, 9187−9201

MATERIALS AND METHODS

Materials. MPO purified from human polynuclear leukocytes and 4-aminobenzoic acid hydrazide (ABAH) were purchased from Calbiochem/EMD Biosciences (Gibbstown, NJ). Amplex Red (10-acetyl-3,7-dihydroxyphenoxazine) was purchased from Invitrogen (Carlsbad, CA). Hydrogen peroxide (H_2O_2) and diethylenetriaminepentaacetic acid (DTPA) were obtained from Alfa Aesar (Ward Hill, MA). Reduced glutathione (GSH), 5,5-dimethyl-1-pyrroline *N*-oxide (DMPO), tris[(1-benzyl-1*H*-1,2,3-triazol-4-yl)-methyl]amine, $CuSO_4$, and catalase were from Sigma-Aldrich (St. Louis, MO). Tris(2-carboxyethyl)phosphine (TCEP) and rhodamine-azide (Rh-N3) were from Hampton Research (Aliso Viejo, CA) and Life Technologies (Grand Island, NY), respectively. Fluorophosphonate-TAMRA (serine hydrolase probe) was purchased from Thermo Scientific (Rockford, IL). All reagents were of the highest quality commercially available. Compounds **A**, **C**, and **D** were synthesized according to the published procedure.[16]

Synthesis of 3-(2-Ethoxypropyl)-1*H*-purine-2,6-(3*H*,9*H*)-dione (B). Methyl iodide (0.1 mL, 1.6 mmol) was added to a solution of compound **A** (0.2 g, 0.8 mmol) in a 2:1 H_2O/1 N NaOH mixture (4 mL) at 0 °C (ice/water). The reaction mixture was allowed to warm to room temperature and stir for 3 h. The reaction was quenched with saturated aqueous ammonium chloride and the mixture extracted three times with ethyl acetate. The combined organic extracts were dried over Na_2SO_4, filtered, and concentrated under reduced pressure to give 3-(2-ethoxypropyl)-2-(methylthio)-3*H*-purin-6(9*H*)-one (0.2 g, 94%). This compound which was used without further purification was dissolved in acetic acid (5.5 mL) at room temperature. A solution of 30% H_2O_2 (0.6 mL) was added dropwise. The reaction mixture was heated at 60 °C for 3 h, cooled to room temperature, diluted with toluene (5 mL), and concentrated under reduced pressure to give a solid. This solid was washed with H_2O and hexanes and then was added to a solution of toluene. The mixture of the solid in toluene was concentrated under reduced pressure to give a solid that was washed with ether and hexanes, yielding 55 mg of **B** (32%): MS M + 1 = 239.4; ^{1}H NMR (400 MHz, DMSO-d_6) δ 13.48 (bs, 1 H), 11.10 (s, 1 H), 8.00 (s, 1 H), 4.02 (bs, 1 H), 3.84−3.82 (m, 2 H), 3.47−3.44 (m, 2 H), 1.07 (bs, 3 H), 0.97 (s, 3 H).

Synthesis of 3-[2-(Prop-2-yn-1-yloxy)ethyl]-2-thioxo-1,2,3,7-tetrahydro-6*H*-purin-6-one (E). To a solution of oxalyl chloride (0.31 mL, 3.6 mmol) dissolved in CH_2Cl_2 (15 mL) and cooled to −78 °C was added DMSO (0.51 mL, 7.2 mmol). After 10 min at −78 °C, 2-(prop-2-yn-1-yloxy)ethanol (300 mg, 3.0 mmol) was added and the mixture stirred for 10 min at −78 °C before Et_3N (1.25 mL, 9.0 mmol) was added. After 10 min at −78 °C, the reaction mixture was warmed to 0 °C. After 0.5 h at 0 °C, the reaction mixture was treated with a 1:1 solution of saturated aqueous ammonium chloride and water. The layers were separated, and the aqueous layer was extracted twice with CH_2Cl_2 before the combined organic layers were washed with brine and dried over Na_2SO_4. The resulting solution was combined with 4-amino-1*H*-imidazole-5-carboxamide (120 mg, 0.74 mmol) dissolved in methanol (3.4 mL). After the mixture was stirred at room temperature for 0.5 h, acetic acid (0.084 mL, 1.5 mmol) was added. After an additional 0.5 h, $NaBH_3CN$ (46 mg, 0.74 mmol) was added. After being stirred at room temperature overnight, the reaction mixture was concentrated under reduced pressure, and the resulting residue was purified by column chromatography on silica (10 g) eluting with a gradient of 0 to 12% methanol in CH_2Cl_2 to afford 101 mg of 4-{[2-(prop-2-yn-1-yloxy)ethyl]-amino}-1*H*-imidazole-5-carboxamide: MS M + 1 = 209; ^{1}H NMR (400 MHz, methanol-d_4) δ 3.43 (t, J = 5.3 Hz, 2 H), 3.66 (t, J = 5.3 Hz, 2 H), 4.17 (d, J = 2.1 Hz, 2 H), 7.24 (s, 1 H). This product (91 mg, 0.44 mmol) was dissolved in CH_2Cl_2 (2 mL) under an inert atmosphere and stirred at room temperature as ethyl isothiocyanatoformate (0.059 mL, 0.525 mmol) was added. After being stirred at room temperature overnight, the reaction mixture was treated with water, and the resulting mixture was concentrated under reduced pressure. The resulting residue was purified by column chromatography on silica (10 g) eluting with a gradient of 0 to 10% methanol in CH_2Cl_2 to afford 118 mg of ethyl {(5-carbamoyl-1*H*-imidazol-4-yl)[2-(prop-2-yn-1-yloxy)-ethyl]carbamothioyl}carbamate: MS M + 1 = 340; ^{1}H NMR (400 MHz, methanol-d_4) δ 1.19 (t, J = 6.0 Hz, 3 H), 3.77 (t, J = 5.3 Hz, 2 H), 4.04−4.12 (m, 4 H), 4.13−4.26 (m, 2 H), 7.71 (s, 1 H). This material (115 mg, 0.34 mmol) was combined with a 1 N aqueous sodium hydroxide solution (0.68 mmol, 0.68 mL) in a microwave vial and heated to 100 °C for 0.3 h in a microwave reactor. After the reaction mixture had cooled, a 1 N aqueous hydrochloric acid solution was added to adjust the pH of the reaction mixture to 7.0. The resulting solid was collected by vacuum filtration, washed with water, and purified by column chromatography on silica (10 g) eluting with a gradient of 0 to 20% methanol in CH_2Cl_2 to afford 24 mg of 3-[2-(prop-2-yn-1-yloxy)ethyl]-2-thioxo-1,2,3,7-tetrahydro-6*H*-purin-6-one (**E**): MS M + 1 = 251; ^{1}H NMR (400 MHz, DMSO-d_6) δ 3.38 (t, J = 2.3 Hz, 1 H), 3.83 (t, J = 6.3 Hz, 2 H), 4.15 (d, J = 2.3 Hz, 2 H), 4.63 (t, J = 6.2 Hz, 2 H), 8.13 (s, 1 H).

MPO Activity Assay. MPO peroxidase activity was measured by monitoring the formation of resorufin generated from the oxidation of Amplex Red by MPO.[17] In the presence of H_2O_2, native MPO is oxidized to compound I. Amplex Red reacts with MPO compound I and undergoes a two-electron oxidation (via compound II) regenerating native MPO and producing the highly fluorescent oxidized product resorufin. Assay mixtures (total volume of 100 μL) contained 50 mM NaP_i (pH 7.4), 150 mM NaCl, 1 mM DTPA, 2% DMSO, the indicated concentrations of H_2O_2, and Amplex Red. The reactions were initiated by the addition of 100 pM MPO. All assays were performed in 96-well, black, half-area, nonbinding surface, polystyrene plates (Corning, Tewksbury, MA). Fluorescent changes [relative fluorescent units per second (RFU/s)] were monitored at room temperature (RT) every 20 s on a Spectramax M2 Microplate Spectrophotometer (Molecular Devices, Palo Alto, CA) equipped with Softmax Pro (Molecular Devices) with excitation and emission filters set at 530 and 580 nm, respectively. Reaction mixtures for determining the background reaction rate consisted of all assay components and 4 μL of 500 unit/mL catalase in 50 mM KP_i (pH 7.0). The background rate was subtracted from each reaction progress curve. All data were analyzed using nonlinear regression analysis in Microsoft Excel and Kaleidagraph (Synergy Software, Reading, PA).

Determination of K_m and k_{cat} Values for H_2O_2 and Amplex Red. To determine the K_m and k_{cat} values for H_2O_2 and Amplex Red, all assay components, including 50 mM NaP_i (pH 7.4), 150 mM NaCl, 1 mM DTPA, 2% DMSO, H_2O_2, and Amplex Red, in a volume of 80 μL were added to the assay plate and mixed on a plate shaker. Assays to determine the K_m for H_2O_2 contained 300 μM Amplex Red and 0.25−10 μM H_2O_2. Assays to determine the K_m for Amplex Red contained 4 μM H_2O_2 and 2.5−500 μM Amplex Red. Reactions were initiated by the addition of 20 μL of 500 pM MPO in 50 mM NaP_i (pH 7.4)

dx.doi.org/10.1021/bi401354d | *Biochemistry* 2013, 52, 9187−9201

and 150 mM NaCl (final MPO concentration of 100 pM); solutions were mixed for 30 s on a plate shaker, and fluorescence changes were immediately monitored. A standard curve was generated using resorufin (Sigma-Aldrich) to convert the fluorescence units (RFU) into micromolar units. All assay components (2 μM H_2O_2 and 300 μM Amplex Red) except MPO were added to the assay plate with 20 μL of varying concentrations of resorufin in water (final concentration from 0 to 0.7 μM), and the fluorescence was read with excitation at 530 nm and emission at 580 nm. The K_m values for Amplex Red and H_2O_2 were determined by plotting the initial reaction rates from the first ~200 s of the linear reaction progress curves (V_o, in micromolar per second) as a function of substrate concentration ([S]) and fitting to the Michaelis−Menten equation (eq 1)

$$V_0 = \frac{V_{max}[S]}{K_m + [S]} \quad (1)$$

where V_{max} (micromolar per second) is the maximal rate of the reaction and K_m is the concentration of substrate required to reach $^1/_2V_{max}$. The k_{cat} value was calculated by dividing the V_{max} by the concentration of MPO in the reaction (100 pM).

Determination of Inhibitor Potency (k_{inact}/K_I ratios and IC_{50} values). To determine the inhibitor potency (k_{inact}/K_I ratios), 20 μL of inhibitor in 10% DMSO was added to the assay plate followed by 60 μL of assay mix consisting of 50 mM NaP_i (pH 7.4), 150 mM NaCl, 1 mM DTPA, 2 μM H_2O_2, and 30 μM Amplex Red and mixed for 5 min on a plate shaker. Reactions were initiated by the addition of 20 μL of 500 pM MPO in 50 mM NaP_i (pH 7.4) and 150 mM NaCl (final MPO concentration of 100 pM); solutions were mixed for 30 s on a plate shaker, and fluorescence changes were immediately monitored. The first ~600 s of the reaction progress curves corresponding to the linear range of the DMSO control was fit to eq 2

$$\text{product} = \frac{V_0}{k_{obs}}[1 - \exp(-k_{obs}t)] \quad (2)$$

where V_0 is the initial rate in RFU/s and t is the time in seconds, yielding the first-order rate constant for enzyme inactivation (k_{obs}) at each inhibitor concentration. Each k_{obs} value was corrected for autoinactivation of the enzyme by subtracting the k_{obs} value for the uninhibited reaction. The corrected k_{obs} values were then plotted versus inhibitor concentration ([I]) and fit to eq 3

$$k_{obs} = \frac{k_{inact}[I]}{K_I + [I]} \quad (3)$$

where k_{inact} is the maximal rate of inactivation and K_I is the inhibitor concentration that yields half the rate of maximal inactivation.[18]

The IC_{50} values were determined by plotting the initial rates (from the first linear ~300 s of each reaction progress curve) as a percentage of the control relative to the uninhibited reaction as a function of inhibitor concentration. The data were fit to eq 4

$$y = \frac{100}{1 + (x/IC_{50})^z} \quad (4)$$

where IC_{50} is the inhibitor concentration at 50% inhibition and z is the Hill slope (the slope of the curve at its inflection point).

Rapid Dilution Reversibility Studies and Determination of the Partition Ratio. A rapid dilution experiment was conducted to assess the reversibility of **A**. Assay mixtures (total volume of 150 μL) contained 50 mM NaP_i (pH 7.4), 1 mM DTPA, 6 μM **A** (20-fold greater than the IC_{50} value), or DMSO in the presence or absence of 2 μM H_2O_2, and the reaction was initiated by the addition of 30 nM MPO. After preincubation for 15 min, 5 μL of the MPO/inhibitor mixture was diluted 300-fold into the MPO assay mixture consisting of 50 mM NaP_i (pH 7.4), 1 mM DTPA, 2 μM H_2O_2, and 30 μM Amplex Red. The final DMSO concentration was kept at 2%. The reaction mixture was vortexed to mix; 100 μL was transferred to an assay plate, and fluorescence changes were monitored as described in MPO Activity Assay.

Partition ratio experiments were performed in a manner identical to that of the rapid dilution experiments with the exception that 60 nM MPO was used, the concentrations of inhibitors were varied in 1.5-fold increments from 0.026 to 15 μM, and 2 μM H_2O_2 was always included in the preincubation. The initial rate of each reaction corresponding to the first linear ~200 s (in RFU/s) was determined from the reaction progress curve. To determine the partition ratio, the percent control activity was plotted as a function of the ratio of the concentration of inhibitor to MPO ([inhibitor]/[MPO]). In this plot, the percent control activity decreases linearly with an increasing [inhibitor]/[MPO] ratio. The point at which this line intersects the x-axis (corresponding to 0% activity) is equal to 1 + r, where r is the partition ratio.

MPO Spectral Scan Analysis. Spectral scans of MPO were performed on a Cary 50 UV−vis spectrophotometer (Varian) using 1 μM MPO in 50 mM NaP_i (pH 7.4) in the presence or absence of 30 μM **A** in a total volume of 100 μL. H_2O_2 titrations (0−160 μM) were conducted with sequential 1 μL additions to the 100 μL reaction mixture in the cuvette. The small, 1 μL volume was used to limit dilution effects in the cuvette during the titration. Absorbance readings were recorded every nanometer from 700 to 350 nm. Difference spectra for each concentration of H_2O_2 were obtained by subtracting out the spectrum for native MPO in the absence of H_2O_2.

Competition of A with the Amplex Red Substrate. Experiments to determine if **A** is competitive with the Amplex Red substrate were performed using the Amplex Red activity assay with a few modifications. The assay mixture (80 μL) consisting of 50 mM NaP_i (pH 7.4), 1 mM DTPA, 150 mM NaCl, 2 μM H_2O_2, 37.5−300 μM Amplex Red, and 1 μM **A** (or DMSO as a control) was added to the assay plate and thoroughly mixed on a plate shaker. Amplex Red and **A** were each added as 10 μL of a 10% DMSO solution. Reactions were initiated by the addition of 20 μL of 500 pM MPO in 50 mM NaP_i (pH 7.4) and 150 mM NaCl (final MPO concentration of 100 pM); the solution was mixed for 30 s on a plate shaker, and fluorescence changes were immediately monitored. Reaction mixtures for determining the background reaction rate at each concentration of Amplex Red consisted of all assay components with 4 μL of 500 units/mL bovine catalase (Sigma) in 50 mM KP_i (pH 7.0). The background rate was subtracted from the reaction progress curves with the corresponding concentration of Amplex Red.

The first ~500 s of the reaction progress curves corresponding to the linear range of the DMSO control was fit to eq 2 to determine the k_{obs} value for the inhibited (1 μM **A**) and uninhibited (DMSO control) reactions at each concentration of Amplex Red. Each k_{obs} value was corrected for autoinactivation of the enzyme by subtracting the k_{obs} value for the uninhibited (DMSO) reaction. To determine k_{inact} and K_I values, the corrected k_{obs} values were plotted versus the concentration of Amplex Red divided by the K_m for Amplex Red ([Amplex Red]/K_m). The data then were fit to eq 5

$$k_{obs} = \frac{k_{inact}}{1 + \frac{K_I}{[I]}\left(1 + \frac{[S]}{K_m}\right)} \quad (5)$$

where k_{obs} is the first-order rate constant for enzyme inactivation, k_{inact} is the maximal rate of inactivation at an infinite concentration of inhibitor, K_I is the inhibitor concentration that yields half the rate of maximal inactivation, [I] is the concentration of **A**, [S] is the concentration of Amplex Red, and K_m is the K_m for Amplex Red.[18]

Transient State Kinetic Analysis of MPO with A. All transient state kinetic experiments were performed on a SF-2004 stopped-flow instrument (Kintek Corporation, Austin, TX) equipped with a photodiode detector for monitoring changes in absorbance and a temperature-controlled water bath set to 25 °C. All concentrations reported are final concentrations. For reactions for monitoring MPO compound I formation, 1 μM MPO in 50 mM NaP_i (pH 7.4) and 1 mM DTPA was loaded into syringe A and H_2O_2 (0−20 μM) in 50 mM NaP_i (pH 7.4) and 1 mM DTPA was loaded into syringe C. The components of syringes A and C were rapidly mixed in the stopped-flow instrument, and the decrease in absorbance (corresponding to MPO compound I formation) was monitored at 429 nm for 100 ms. The reaction progress curves for each concentration of H_2O_2 were fit to a single-exponential function (eq 6)

$$\text{absorbance} = A\ \exp(-k_{obs}t) + C \quad (6)$$

where A is the amplitude, k_{obs} is the observed rate constant for the formation of compound I, t is the time in seconds, and C is the y-intercept. The k_{obs} values were then plotted as a function of H_2O_2 concentration and fit to a linear equation in which the slope of the line is equal to the second-order rate constant k_1 for the generation of compound I (Scheme 1).

Scheme 1

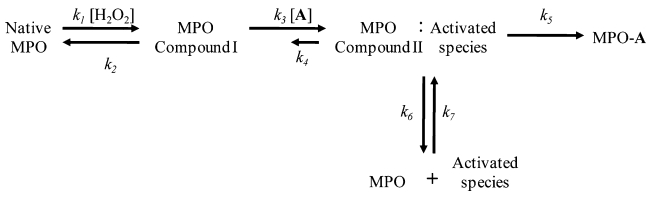

Sequential mixing experiments were used to monitor the formation of MPO compound II resulting from the reaction of **A** with compound I. MPO (1 μM) in 50 mM NaP_i (pH 7.4) and 1 mM DTPA was loaded into syringe A, and 10 μM H_2O_2 in 50 mM NaP_i (pH 7.4) and 1 mM DTPA was loaded into syringe B. Syringe C contained varying concentrations of **A** (0−50 μM) in 50 mM NaP_i (pH 7.4) and 1 mM DTPA. For each reaction, syringe A and syringe B were initially mixed in the delay line of the stopped flow for 70 ms for the complete formation of compound I followed by the addition of the contents of syringe C. MPO compound II formation was monitored at 456 nm for 3 s. The reaction progress curves were fit to eq 6 to obtain the observed rate constant k_{obs} for the formation of compound II. The k_{obs} values were plotted as a function of **A** concentration, and the data were fit to a linear equation in which the slope of the line is equal to the second-order rate constant k_3 for the formation of compound II (Scheme 1).

Preparation of Liver Proteomes. XTreme 200 pooled human liver *S*9 fractions (lot number 0810405) were purchased from Xenotech (Lenexa, KS) and centrifuged at 100000*g* for 1 h at 4 °C. The resulting supernatant was saved as the human soluble proteome. Livers were harvested from wild-type C57Bl/6J mice and immediately frozen in liquid N_2. The livers were then lysed in PBS buffer (20 mL/g of tissue) using a TissueLyser (Qiagen) at a frequency of 30 s^{-1} for 5 min. Cell debris was removed by centrifugation at 1000*g* for 10 min at 4 °C. The supernatant was centrifuged at 100000*g* for 1 h at 4 °C, and this supernatant was saved as the mouse soluble proteome.

CC Analysis of MPO and Proteomes with an Alkyne Analogue E. MPO (1 μM), the indicated concentrations of the soluble liver proteomes from human or mouse, or a mixture of MPO and aforementioned proteomes was incubated with 10 μM **E**, an alkyne analogue of **A**, in the absence or presence of the indicated concentrations of H_2O_2 in PBS in a total volume of 75 μL at RT for 30 min. For competition experiments with the parent inhibitor **A**, 200 μM **A** was added and the mixture incubated at RT for 30 min prior to the addition of **E**. Catalase (5 μL of a 0.1 mg/mL stock) was added, and the resulting mixture was further incubated at RT for 1 h to remove the remaining H_2O_2 from the reaction mixtures. This was followed by CC reaction as previously described with 50 μM rhodamine-azide (Rh-N_3, 2 μL of a 2.5 mM solution in DMSO), 1 mM TCEP (2 μL of a 50 mM solution in H_2O), 100 μM ligand {tris[(1-benzyl-1*H*-1,2,3-triazol-4-yl)methyl]amine} (6 μL of a 1.67 mM solution in 20% DMSO/80% in *tert*-butanol), and 1 mM $CuSO_4$ (10 μL of a 10 mM solution in H_2O) in a total volume of 100 μL.[19,20] The reactions were allowed to proceed at RT for 1 h with vortexing every 15 min before being quenched with 35 μL of 4× sodium dodecyl sulfate−polyacrylamide gel electrophoresis (SDS−PAGE) loading buffer (reducing). Quenched reaction mixtures were subjected to SDS−PAGE on a 12% NuPAGE Bis-Tris gel (Invitrogen) under reducing conditions (15 μL per lane) and visualized in gel with a Typhoon Trio flatbed fluorescence scanner (GE Healthcare, Piscataway, NJ).

Western Blot Analysis of ApoA1. Recombinant ApoA1 (Cell Sciences, Canton, MA) (5 μM) was incubated with 57 nM MPO and 30 μM **A** (or DMSO as a control) in 50 mM NaP_i (pH 7.4), 150 mM NaCl, and 1 mM DTPA for 5 min, and the reaction was initiated by the addition of 35.5 μM H_2O_2 in a total reaction volume of 30 μL. **A** was added in 10% DMSO, and the final DMSO concentration was 1%. Control reactions were also run without MPO and without H_2O_2. Reaction mixtures were incubated at RT for 2 h and then subjected to SDS−PAGE on a 4 to 12% NuPAGE Bis-Tris gel under reducing conditions. Western blot analysis was performed using a goat anti-human ApoA1 primary antibody (1:1000 dilution, Diasorin, Stillwater, MN) and a rabbit anti-goat secondary antibody (1:15000 dilution, Pierce, Rockford, IL). The Western blot was visualized using the Super-Signal West Pico Chemiluminescent Substrate kit (Pierce).

RESULTS

Inhibition of MPO by A. To establish MPO assay conditions for inhibitor characterization, we utilized the Amplex Red assay[17] and first determined the K_m and k_{cat} values for the H_2O_2 and Amplex Red substrates. Under the conditions described in Materials and Methods, substrate inhibition was observed with H_2O_2 concentrations greater than ∼5 μM as shown in the inset of Figure 2A. H_2O_2 substrate inhibition has been previously reported for MPO and proposed to be a result of H_2O_2-dependent destruction of the heme group or generation of inactive MPO compound III at high H_2O_2 concentrations.[21−23] The Michaelis−Menten plots for the determination of K_m and k_{cat} values for both H_2O_2 and Amplex Red are shown in panels A and B of Figure 2,

dx.doi.org/10.1021/bi401354d | *Biochemistry* 2013, 52, 9187−9201

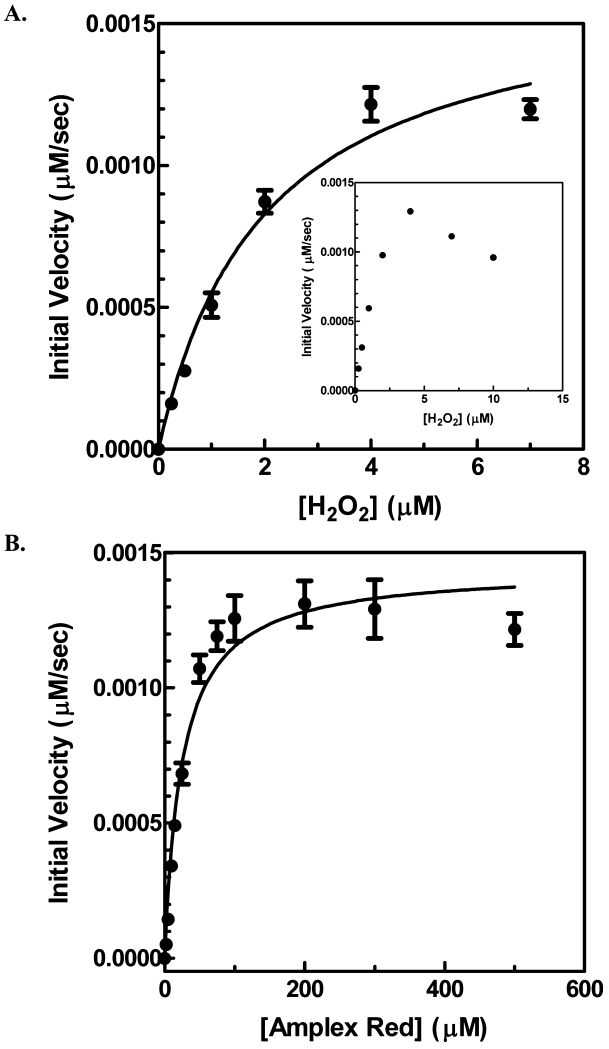

Figure 2. Determination of MPO K_m values for H_2O_2 (A) and Amplex Red (B). The MPO reactions were conducted with 100 pM MPO, and the initial reaction rates were determined using the reaction progress curves as described in Materials and Methods. Data are averages, and error bars represent the SD from three separate experiments. (A) The H_2O_2 concentrations were varied from 0.25 to 10 μM with a saturating Amplex Red concentration of 300 μM. Substrate inhibition by H_2O_2 was observed at >5 μM H_2O_2 (inset), and therefore, the data for 0.25−7 μM H_2O_2 were included in the K_m value determination. The initial rates were plotted as a function of H_2O_2 concentration, and the data were fit to eq 1. The K_m and k_{cat} values for H_2O_2 were determined to be 1.99 ± 0.46 μM and 16.6 ± 1.5 s^{-1}, respectively. (B) The Amplex Red concentrations were varied from 2.5 to 500 μM with 4 μM H_2O_2 (where no substrate inhibition by H_2O_2 was observed). The initial rates were plotted as a function of Amplex Red concentration, fit to eq 1. The K_m and k_{cat} values for Amplex Red were determined to be 25.1 ± 4.4 μM and 14.2 ± 0.66 s^{-1}, respectively.

respectively. The K_m and k_{cat} values for H_2O_2 using H_2O_2 concentrations of <7 μM were determined to be 1.99 ± 0.46 μM and 16.6 ± 1.5 s^{-1}, respectively, at a saturating Amplex Red concentration (300 μM). The K_m and k_{cat} values for Amplex Red were measured at 4 μM H_2O_2, where no substrate inhibition was detected, and were determined to be 25.1 ± 4.4 μM and 14.4 ± 0.66 s^{-1}, respectively. The MPO catalytic efficiencies (k_{cat}/K_m values) for H_2O_2 and Amplex Red substrates were 8.34×10^6 and 0.57×10^6 M^{-1} s^{-1}, respectively. For the inhibitor characterization studies, MPO reactions were conducted with both substrate concentrations approximately at K_m values (2 μM H_2O_2 and 30 μM Amplex Red).

Next, we examined MPO inhibition by **A**, the thioxanthine analogue (Figure 1A) that has been recently described.[15,16] As shown in Figure 3A, the MPO reaction is linear over a 600 s time period in the absence of **A**. In the presence of **A**, the progress curves for the Amplex Red conversion to resorufin by MPO in the presence of H_2O_2 exhibited curvature and time-dependent inhibition as typically expected from an irreversible mechanism of inhibition. The data were fit to eq 2 as described in Materials and Methods to determine the pseudo-first-order rate constant k_{obs}, the rate of inactivation at each inhibitor concentration. Plotting these k_{obs} values as a function of the concentration of **A**, as described in eq 3, revealed saturable inactivation kinetics indicating a two-step mechanism of inactivation (Figure 3B). The k_{inact} and K_I values for **A** were determined to be 0.00347 ± 0.00014 s^{-1} and 413 ± 54 nM, respectively. The resulting inhibitor potency k_{inact}/K_I ratio was 8450 ± 780 M^{-1} s^{-1} (Figure 3B and Table 1). We also obtained an IC_{50} value of 315 ± 17 nM for MPO inhibition by **A** using initial rates from the first 300 s of the reaction at each inhibitor concentration (Figure 3C). We next assessed the importance of sulfur in the thioxanthine ring in **A** for MPO inhibition. Compound **B** is the xanthine analogue of **A** and has a structure identical to that of **A** except sulfur has been replaced with oxygen (Figure 1A). As shown in Figure 3C, **B** exhibited no MPO inhibition up to 100 μM, indicating the sulfur in the thioxanthine ring of **A** is critical for MPO inhibition. Compound **A** is a mixture of two stereoisomers. To determine if only one enantiomer is responsible for MPO inhibition, we synthesized both stereoisomers (compounds **C** and **D**) (Figure 1B) and assessed them for MPO inhibition. As shown in Table 1, **A**, **C**, and **D** all have comparable potencies, indicating that both stereoisomers equally inhibit MPO. Therefore, a racemic mixture **A** was used for all experiments described below.

Rapid Dilution Studies Confirm That MPO Inhibition by A Is Irreversible and H_2O_2-Dependent. To verify that the inhibition of MPO by **A** is irreversible and requires H_2O_2, we performed rapid dilution experiments in the presence and absence of H_2O_2. MPO (30 nM) was preincubated in the presence of 2 μM H_2O_2 with 6 μM **A**, a concentration approximately 20-fold higher than the IC_{50} value, or DMSO as a control for 15 min at RT. After preincubation for 15 min, the reaction mixture was rapidly diluted 300-fold into the assay buffer containing both H_2O_2 and Amplex Red substrates and the resulting MPO activity was immediately monitored. As shown in Figure 4, no recovery of MPO activity was observed with **A** when H_2O_2 was included in the preincubation mixture, confirming that **A** is an irreversible inhibitor.

Mechanism-based inactivation is a specific type of irreversible inhibition in which a nonreactive compound is recognized by the enzyme as a "pseudosubstrate" and via enzyme catalysis is transformed into an activated species that inhibits the enzyme.[18] One of the requirements for classifying an inhibitor as a mechanism-based inactivator is demonstrating that catalysis is required for inhibition. For this purpose, we assessed the requirement of H_2O_2 for MPO inhibition by **A**. We performed the rapid dilution experiment without H_2O_2 in the preincubation. Without the substrate H_2O_2 in the preincubation, enzyme catalysis is not possible, and we would not expect to observe inhibition by **A** if it is a mechanism-based inactivator of MPO. As shown in Figure 4, no inhibition was observed with **A** when H_2O_2 was excluded from the preincubation. This result demonstrates that MPO inhibition by **A** depends on the substrate H_2O_2,

dx.doi.org/10.1021/bi401354d | Biochemistry 2013, 52, 9187−9201

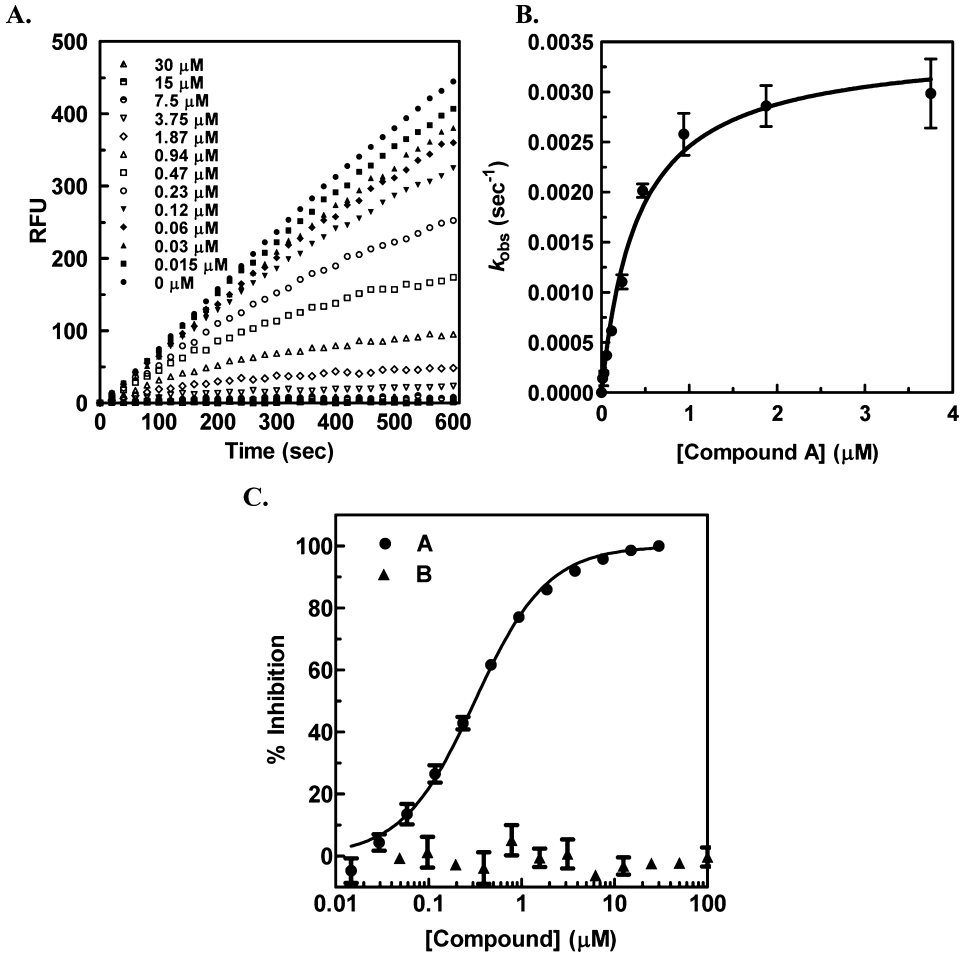

Figure 3. Determination of inhibitor potency. The MPO reactions were conducted as described in Materials and Methods. Data are averages, and error bars represent the SD from three separate experiments. (A) MPO inhibition progress curves show time-dependent inhibition by **A**. The concentrations of **A** were varied from 0.015 to 30 μM. The k_{obs} value from each inhibitor concentration was obtained by fitting the time courses to eq 2 as described in Materials and Methods. (B) The k_{obs} values were plotted as a function of compound **A** concentration, and the data were fit to eq 3 to determine the kinetic inhibition constants k_{inact} and K_I values. (C) The data were plotted as a percentage of inhibition vs inhibitor concentration and fit to eq 4 to determine the IC_{50} value. The concentrations of **B** were varied from 0.048 to 100 μM. No inhibition was observed at up to 100 μM **B**.

Table 1. Inhibition Constants for MPO Inhibitors[a]

compd	k_{inact} (s^{-1})	K_I (nM)	k_{inact}/K_I (M^{-1} s^{-1})
A	0.00347 ± 0.00014	413 ± 54	8450 ± 780
C	0.00532 ± 0.00031	546 ± 95	9760 ± 1300
D	0.00362 ± 0.00033	429 ± 120	8430 ± 950

[a]Inhibition constants were determined as described in Materials and Methods using varying inhibitor concentrations from 0.014 to 30 μM. The average of three experiments with the standard error of the fit is shown.

indicating that **A** could act as an irreversible mechanism-based inhibitor.

Heme Spectral Analysis Demonstrates That A Acts as a Peroxidase Substrate of MPO. MPO has a complex catalytic cycle involving multiple redox intermediates. In the halogenation cycle, the native enzyme [Fe(III) Por] reacts with H_2O_2 and undergoes a two-electron oxidation forming compound I [Fe(IV)═O $Por^{•+}$ (reaction I)]. Compound I is a strong oxidant that readily reacts with chloride (or other halides) and through a two-electron reduction reaction produces hypochlorous acid (HOCl or HOX), simultaneously regenerating the native enzyme (reaction II). Alternatively, in the peroxidase cycle, compound I reacts with various organic or inorganic peroxidase substrates.

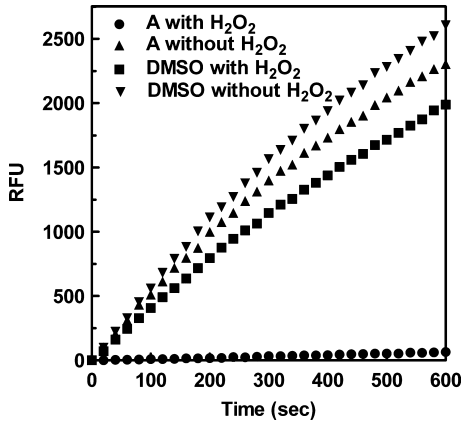

Figure 4. Reversibility of MPO inhibition by **A** in the presence or absence of H_2O_2. MPO was incubated with **A** at 5 μM (20-fold greater than the IC_{50} value) or DMSO with or without 2 μM H_2O_2. After 15 min, an aliquot of the preincubation mixture was diluted 300-fold into MPO assay buffer containing 2 μM H_2O_2 and 30 μM Amplex Red and the reaction was immediately monitored as described in Materials and Methods.

A one-electron oxidation of the peroxidase substrate by compound I generates compound II [Fe(IV)═O Por (reaction III)].

dx.doi.org/10.1021/bi401354d | *Biochemistry* 2013, 52, 9187−9201

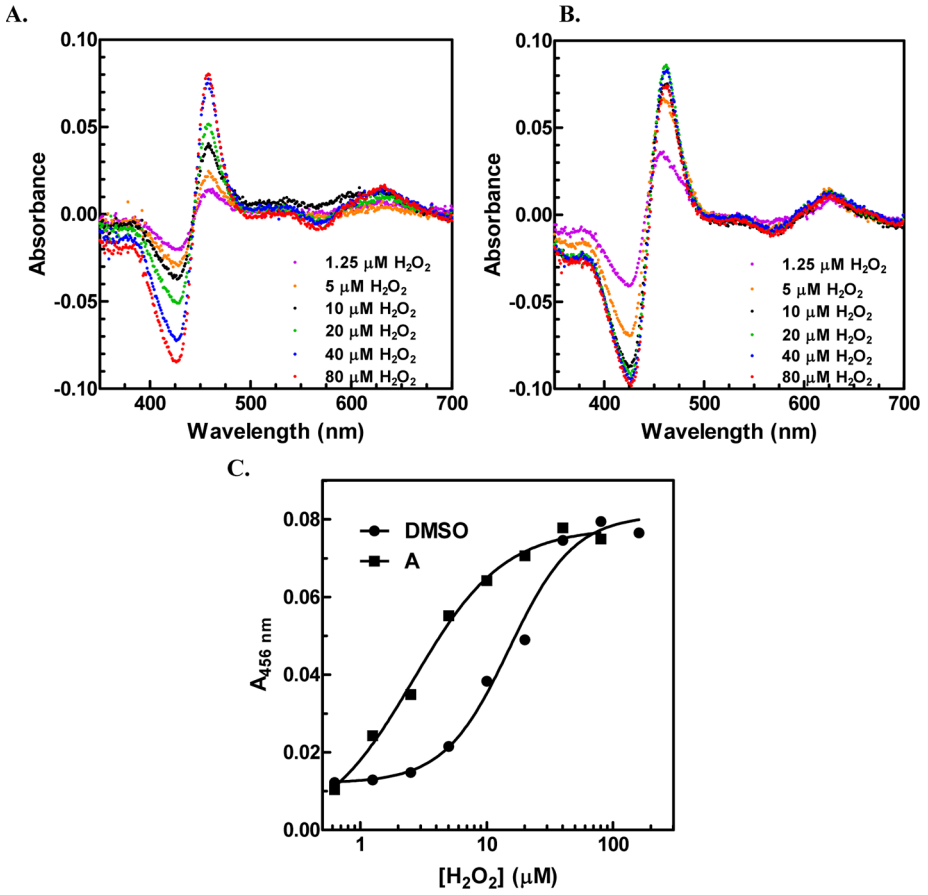

Figure 5. Heme spectral analysis for the assessment of the interaction of MPO with **A**. The absorbance spectrum of MPO was recorded with increasing concentrations of H_2O_2 (0−160 μM) in the absence (A) or presence (B) of 30 μM **A**. Representative difference spectra are reported, and compound II formation is indicated by the peak at 456 nm. No changes were observed upon addition of **A** in the absence of H_2O_2. (C) Absorbance at 456 nm from the spectra in panels A and B was plotted as a function of H_2O_2 concentration. The data were fit to the equation $y = y_{min} + (y_{max} - y_{min})/[1 + (EC_{50}/x)^z]$, where EC_{50} is the H_2O_2 concentration at 50% of the maximal absorbance at 456 nm and z is the Hill slope, to determine the EC_{50} values for compound II formation. The H_2O_2 concentration required for compound II formation in the presence of **A** is ~6-fold lower than that in the absence of **A**, indicating that **A** is reacting with compound I by acting as a peroxidase substrate for MPO.

A successive one-electron reduction of compound II regenerates the native enzyme (reaction IV). Compound II can also be formed at high concentrations of H_2O_2 in the absence of halides or peroxidase substrates. MPO has additional redox intermediate states, the ferrous [Fe(II) Por] state and compound III [Fe(III)-$O_2^{\bullet-}$ Por] that do not participate in the halogenation or peroxidation cycle.[1,2,13,24,25]

The spectral properties of the MPO redox intermediates are well documented in the literature and are useful for monitoring the various states of the enzymatic reaction.[24,25] The native enzyme is characterized by a peak of maximal absorbance at 429 nm, and compound I is detected by a hypochromicity of that same peak at 429 nm. Compound II is distinguished by a shift of the 429 nm peak to 456 nm, and the ratio of the absorbance at 625 and 456 nm (A_{625}/A_{456}) of 0.17 is used as an indication of complete compound II formation. Compound III is distinguished by an A_{625}/A_{456} of 0.52.[24]

Our rapid dilution experiments showing the requirement of H_2O_2 for MPO inhibition by **A** indicated that MPO catalysis is required for inhibition by **A**. To provide additional evidence to show that **A** is reacting with MPO as a peroxidase substrate, we used spectral scan analysis and monitored the redox intermediates and catalytic cycle of MPO. Absorbance scans of MPO were measured with increasing concentrations of H_2O_2 in the presence and absence of 30 μM compound **A**. The difference spectra of 1 μM MPO in the presence of increasing concentrations of H_2O_2 are shown in Figure 5A. As expected on the basis of previously published studies,[24] in the absence of halides or a peroxidase substrate, a near complete formation of compound II was observed upon addition of 40−80 μM H_2O_2 as indicated by the peak at 456 nm and an A_{625}/A_{456} of 0.21. In the presence of 30 μM **A**, much lower H_2O_2 concentrations of 10−20 μM were sufficient for a full formation of compound II as shown in Figure 5B. In Figure 5C, the absorbance at 456 nm is shown as a function of H_2O_2 concentration and the data were fit to determine EC_{50} values (defined as the H_2O_2 concentration that yields 50% of the maximal absorbance at 456 nm). The resulting EC_{50} values were 15.0 ± 2.1 and 2.61 ± 0.60 μM in the absence and presence of **A**, respectively, which highlight the ~6-fold shift to lower concentrations of H_2O_2 required to form compound II in the presence of **A**. These data indicate that **A** is acting as a peroxidase substrate for MPO. The small amount of H_2O_2 reacts with native MPO to generate compound I that in turn oxidizes **A** with the concomitant conversion of compound I to compound II. Of note, these results indicate that **A** inhibits MPO via a mechanism distinct from that of the known MPO inhibitor 4-aminobenzoic acid hydrazide (ABAH). Spectral scan analysis with ABAH was shown to reveal the formation of compound III,[26]

dx.doi.org/10.1021/bi401354d | *Biochemistry* 2013, 52, 9187−9201

in contrast to compound II formation by **A** as discussed above. Because ABAH is a substrate for both compound I and compound II, it has been proposed that the oxidation of ABAH by compound I and compound II (reactions III and IV) generates radicals that readily react with native MPO, producing compound III via ferrous MPO (reactions V and VI).[26,27]

$$\text{MPO} + {}^{\bullet}\text{AH} \rightarrow \text{ferrous MPO} + \text{A} + \text{H}^{+} \quad \text{(V)}$$

$$\text{ferrous MPO} + \text{O}_2 \rightarrow \text{compound III} \quad \text{(VI)}$$

Our spectral scan analysis data combined with the results described above showing the requirement of H_2O_2 for inhibition and the covalent modification of MPO illustrate that **A** is oxidized by MPO into an activated form that is capable of forming a covalent bond with the heme moiety of the enzyme, resulting in MPO inactivation.

Compound A Is Competitive with the Amplex Red Substrate. Another distinguishing feature of a mechanism-based inactivator is that it should be competitive with one of the substrates of the reaction (because it is acting as a "pseudosubstrate"), and consequently, the substrate should protect against inactivation of the enzyme.[18] The spectral scan analysis suggested that **A** is acting as a peroxidase substrate for MPO; therefore, it is expected that **A** would be competitive with the Amplex Red substrate in the MPO assay described in Materials and Methods. To test this hypothesis, we monitored MPO activity in the presence of 1 μM **A** at varying concentrations of Amplex Red ranging up to 10-fold over the K_m value. The k_{obs} values for the reactions at various concentrations of Amplex Red were determined. As shown in Figure 6, MPO inactivation

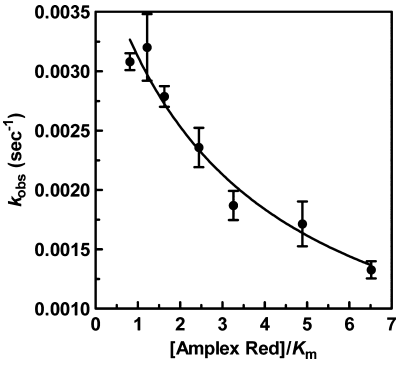

Figure 6. Compound **A** is competitive with the Amplex Red substrate. The MPO reactions were conducted with 100 pM MPO and varying concentrations of Amplex Red (37.5−300 μM) under the conditions described in Materials and Methods. The first ~500 s of each reaction progress curve was fit to eq 2 to determine the k_{obs} value at each concentration of Amplex Red. The k_{obs} values were plotted as a function of the ratio of Amplex Red concentration to the K_m value ([Amplex Red]/K_m) and fit to eq 5 to determine the inhibition constants k_{inact} and K_I. Data are averages, and error bars represent the SD from four separate experiments.

by **A** is protected by the Amplex Red substrate as the observed rate of inactivation (k_{obs}) decreases with increasing concentrations of Amplex Red. The data in Figure 6 were fit to eq 5 to determine k_{inact} and K_I values for **A**. The values for k_{inact} of 0.00586 ± 0.00085 s^{-1} and K_I of 438 ± 12 nM obtained were comparable to those determined using methods described above (see Table 1 and Inhibition of MPO by A), further validating the data from this competition experiment.

Inactivation of MPO by A Occurs Prior to the Release of the Activated Species from the Active Site. As shown in Scheme 1, once the active species forms, it can go on to inactivate the enzyme directly or be released into solution. To be considered a true mechanism-based inhibitor, the specific activated species responsible for MPO inactivation should not dissociate from the enzyme prior to covalent bond formation. To assess whether **A** satisfies this criterion, we measured the potency (k_{inact}/K_I) of **A** in the presence of a trapping agent to scavenge any affinity label or radical species that are produced during the catalytic cycle. DMPO (5,5-dimethyl-1-pyrroline *N*-oxide) and reduced glutathione (GSH) are radical trapping agents that will sequester activated inhibitor molecules once they are released from the enzyme and effectively prevent enzyme inactivation due to any released activated species. For a true mechanism-based inactivator in which the activated species does not dissociate prior to covalent bond formation, the presence of the trapping agent should have no effect on the k_{obs} value or potency of **A**. To measure the potency of **A** in the presence of the trapping agent DMPO, we first confirmed that up to 500 μM DMPO has no effect on MPO activity (data not shown) and then determined the potency of **A** in the presence of DMPO. We observed little change in the inhibition kinetic constants in the presence of DMPO (k_{inact}/K_I of 6550 ± 1800 M^{-1} s^{-1} with DMPO vs 8450 ± 780 M^{-1} s^{-1} without DMPO).

Similarly, GSH was also assessed. As GSH inhibits MPO activity, the maximal concentration of GSH that could be used for this purpose was 10 μM. GSH at 10 μM showed little effect on the potency of **A** for MPO inhibition (data not shown). These results indicate that the activated species responsible for inhibiting MPO does not dissociate from the enzyme prior to covalent bond formation and thus support the idea that **A** is a true mechanism-based inhibitor.

Determination of the Partition Ratio for A. Having determined that **A** meets all the criteria for a mechanism-based inhibitor, we next measured the partition ratio, which is a quantitative assessment of inactivation efficiency or partitioning of the activated inhibitor between direct covalent adduct formation in the enzyme active site and release into solution.[18] As shown in Scheme 1, after **A** becomes activated by MPO, the inhibitory species can either form a covalent bond with the enzyme (described by the rate constant k_5) or be released into solution (governed by the rate constant k_6). To determine the partition ratio (the ratio of first-order rate constants k_6/k_5) for **A**, experiments similar to the rapid dilution experiments described above were conducted. MPO (30 nM) was preincubated with 2 μM H_2O_2 and **A** at concentrations varying by 1.5-fold increments between 0.026 and 15 μM (or DMSO for the control) for 15 min and then rapidly diluted 300-fold into assay buffer containing substrates (2 μM H_2O_2 and 30 μM Amplex Red). The resulting MPO activity was monitored as described in Materials and Methods. The initial velocity for each concentration of **A** was determined from the reaction progress curves and converted to the percentage of control activity. The percentage of control activity was plotted as a function of the ratio of inhibitor versus enzyme ([I]/[E]). As shown in Figure 7, the remaining fractional activity falls off as a linear function of [I]/[E] until there is no activity remaining. The point at which this straight line intersects the *x*-axis was determined to be 16.6, which is equal to one plus the partition ratio assuming a stoichiometry of 1:1 for irreversible inactivation of the enzyme by the activated inhibitor. This means that the complex of MPO and activated inhibitory species goes on to form the

dx.doi.org/10.1021/bi401354d | *Biochemistry* 2013, 52, 9187−9201

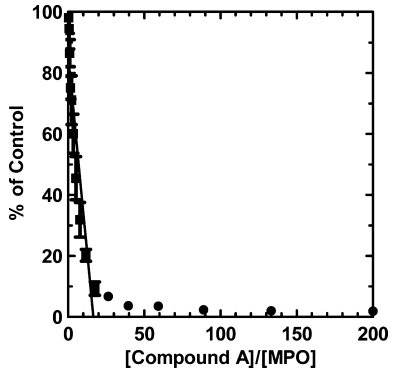

Figure 7. Determination of the partition ratio for **A**. MPO was incubated with 2 μM H_2O_2 and **A** at concentrations varying by 1.5-fold between 0.026 and 15 μM (or DMSO for control). After 15 min, an aliquot of the preincubation mixture was diluted 300-fold into MPO assay buffer with 2 μM H_2O_2 and 30 μM Amplex Red and the reaction was monitored. The initial rate of each progress curve was determined as described in Materials and Methods. The percent control of each inhibited reaction was plotted as a function of the ratio of compound **A** to MPO ([**A**]/[MPO]). Data are averages, and error bars represent the SD from two separate experiments.

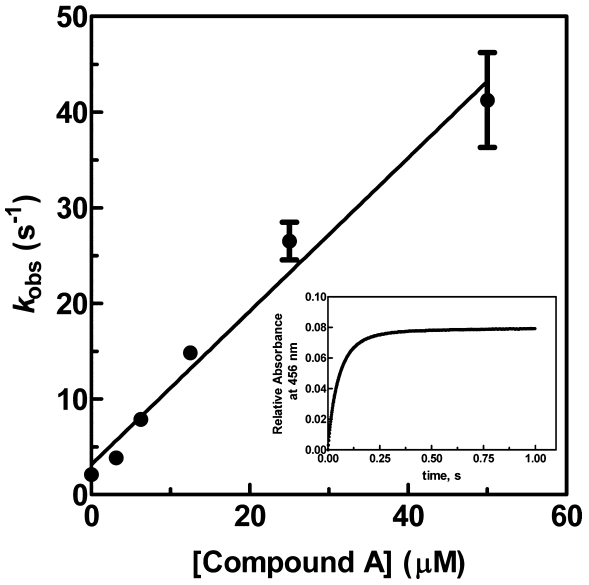

Figure 8. Transient state kinetic analysis of MPO inactivation by **A**. MPO was rapidly mixed with H_2O_2 for 70 ms followed by the rapid addition of 0–50 μM **A** in a stopped-flow instrument (Kintek Corp.), and compound II formation was monitored at 456 nm. The reaction progress curves (inset shown for 12.5 μM **A**) were fit to eq 6 to determine the k_{obs} value for formation of compound II at various concentrations of **A**. The k_{obs} values were plotted as a function of the concentration of **A** and fit to a linear equation to determine the second-order rate constant for the reduction of compound I by **A** [$(0.801 \pm 0.056) \times 10^6$ M^{-1} s^{-1}]. Data are averages, and error bars represent the SD from two separate experiments.

covalent MPO–**A** adduct only one time for every 16.6 turnover events of the MPO reaction with **A**.

Rapid Kinetic Analysis of the Formation of Compound II by A. The MPO spectral analysis indicated that **A** inhibits MPO by acting as a peroxidase substrate and reducing MPO compound I to compound II. To explore this redox reaction in more detail, we performed rapid kinetics using stopped-flow sequential mixing experiments in which native MPO is first rapidly mixed with H_2O_2 to form compound I followed by the addition of **A**. Previous studies have shown that compound I, characterized by a reduced absorbance in the Soret region, is completely formed when native MPO is rapidly mixed with a 10-fold excess of H_2O_2.[13,27] Initially, we determined rate constant k_1 for forming the transient compound I species (reaction I). MPO (1 μM) was rapidly mixed with varying concentrations of H_2O_2 (0–20 μM), and the decrease in absorbance was monitored at 429 nm. The k_{obs} values obtained from fitting the time courses to a single-exponential equation (eq 6) were plotted as a function of H_2O_2 concentration to derive the second-order rate constant for the generation of compound I. The resulting rate constant k_1 of $(0.811 \pm 0.28) \times 10^7$ M^{-1} s^{-1} was comparable to the reported value of 1.4×10^7 M^{-1} s^{-1},[27] and the formation of compound I was complete within 70 ms under these conditions.

Once the optimal condition for generating compound I was determined, a sequential mixing experiment was used to examine the interaction of compound I with **A** governed by rate constant k_3 in reaction III. MPO (1 μM) was premixed with 10 μM H_2O_2 for 70 ms for the complete formation of compound I. This was followed by the addition of varying concentrations of **A** (0–50 μM), and compound II formation was monitored as an increase in absorbance at 456 nm. As described in Materials and Methods, the time courses were best fit to a single-exponential equation (eq 6) (typical time trace and fit at 12.5 μM **A** are shown in the inset of Figure 8), and the resulting rate constants (k_{obs}) were plotted as a function of the concentration of **A** (Figure 8). The linear fit of this plot yielded a second-order rate constant k_3 of $(0.801 \pm 0.056) \times 10^6$ M^{-1} s^{-1} for the reduction of compound I by **A** (Scheme 1). We also assessed the rate constant associated with the reduction of MPO compound I by the known MPO inhibitor ABAH, which has been shown to reduce MPO compound I to compound II. The rate constant k_3 of 6.31×10^6 M^{-1} s^{-1} we obtained for ABAH was comparable to that reported in the literature (3.34×10^6 M^{-1} s^{-1}).[27] It is noteworthy that the rate constant k_3 for **A** is approximately 13-fold slower than that of ABAH. It would be interesting to study how these rate constants relate to the selectivity for MPO versus other peroxidases and other proteins.

A Is Selective against a Broad Panel of 100 Targets. Selectivity assessment is critical in determining whether any compound can serve as a pharmacological tool or drug. Therefore, we assessed the *in vitro* selectivity of compound **A** at 10 μM against a broad panel consisting of binding or functional activity assays for more than 100 targets, including receptors, enzymes, transporters, and ion channels (Table S1 of the Supporting Information). The results shown in Table S2 of the Supporting Information illustrate that **A** is selective as **A** at 10 μM does not inhibit any targets assessed to a significant extent; the highest level of inhibition of 26% was obtained for the sodium channel.

Selectivity of A in Human and Mouse Proteomes. Next, we wanted to determine whether **A** covalently modifies any proteins in liver proteomes derived from human and mouse sources. On the basis of the relatively high partition ratio of 15.6 for **A** we determined above, we wanted to assess whether the activated inhibitory species of **A** generated by MPO is released to form covalent adducts with other proteins, which could potentially lead to off-target effects. To achieve this, we synthesized **E**, an alkyne analogue of **A** (Figure 9A), which maintained a high potency for MPO (k_{inact}/K_I ratio of 5305 M^{-1} s^{-1}) and displayed a partition ratio of 16.4, similar to that of **A** (Figure S1 of the Supporting Information). First, we established reaction

dx.doi.org/10.1021/bi401354d | *Biochemistry* 2013, 52, 9187–9201

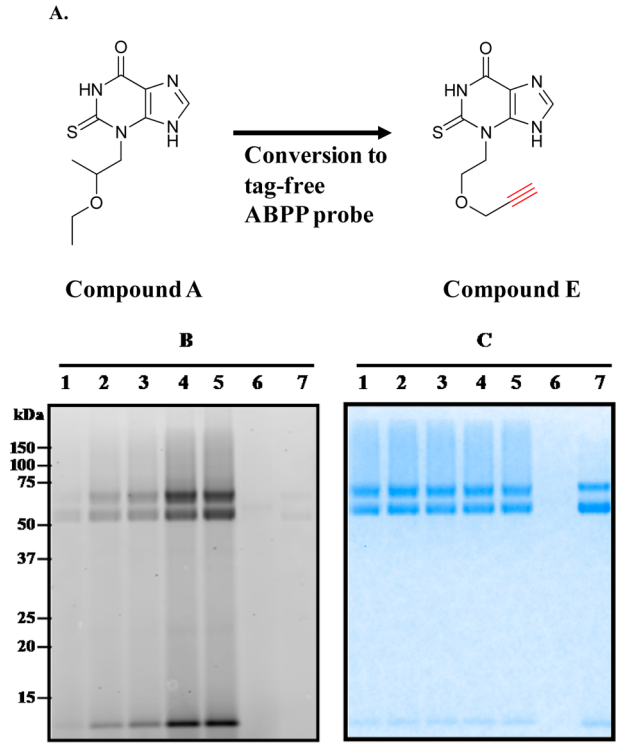

Figure 9. Labeling of purified MPO by an alkyne analogue **E** after CC. (A) Structure of **E**, an alkyne analogue of **A**. (B) Gel profiles of CC–ABPP experiments in which MPO was incubated with **E** at various H_2O_2 concentrations. After the removal of the remaining H_2O_2 by the addition of catalase, the samples were treated with a rhodamine-azide tag under CC conditions and analyzed by in-gel fluorescence scanning (shown in grayscale). Lanes 1–5 contained 0, 5, 10, 30, and 100 μM H_2O_2, respectively. Lane 6 contained catalase alone. Lane 7 contained purified MPO directly loaded onto the gel. (C) The same gel shown in panel B was stained by Coomassie staining.

conditions for monitoring the protein reactivity of **E** using purified MPO. MPO was incubated with **E** at 10 μM in the presence of various concentrations of H_2O_2 to form an MPO–**E** adduct. The reaction mixture was then treated with catalase to remove unreacted remaining H_2O_2, which was followed by treatment with an azide-rhodamine tag under click chemistry (CC) conditions.[19,20] The resulting samples were assessed via SDS–PAGE under reducing conditions and analyzed by in-gel fluorescence scanning. The same gel was then visualized by Coomassie staining. As expected, when MPO was visualized by Coomassie staining after the treatment and CC described above, it showed two bands corresponding to each subunit (running at ~14 and 58 kDa), and one additional band corresponding to two combined subunits (running at ~73 kDa) on SDS–PAGE (Figure 9C). The same three bands were observed with the MPO sample directly run on SDS–PAGE and visualized by Coomassie staining (Figure 9C, lane 7), confirming that MPO labeling by **E** does not alter the mobility of each subunit of MPO on SDS–PAGE. As shown in Figure 9B from the in-gel fluorescence scanning, all three bands of MPO were clearly labeled by **E** with an optimal labeling at 30–100 μM H_2O_2 (Figure 9B, lanes 4 and 5). Because the modification of the heme in MPO by the parent inhibitor **A** has been shown to occur in the heme pyrrole D-ring based on the crystal structure of the MPO–**A** complex,[14,15] it is expected that each subunit that is covalently linked to the heme would contain **E**. As shown in Figure 10A, the labeling of MPO by **E** was H_2O_2-dependent, as little labeling was observed in the absence of H_2O_2 (lane 1) compared to that in the presence of 100 μM H_2O_2 (lane 4). Similarly, minimal labeling was detected when MPO was first incubated with the parent inhibitor **A** prior to labeling by **E** in the presence (lane 3) or absence (lane 2) of H_2O_2, indicating **E** competes for binding to the same site as **A** on the MPO protein. Removal of the remaining H_2O_2 by calatase treatment prior to CC was critical as CC occurred poorly without catalase treatment (data not shown).

We next directly analyzed the protein targets of **E** by CC–ABPP in soluble liver proteomes from human and mouse treated with **E**. Liver proteomes were chosen for this experiment as these proteomes express several heme-containing enzymes. Because MPO is not endogenously expressed in liver proteomes, we attempted to establish optimal proteome conditions under which MPO is labeled by **E** in the presence of varying concentrations of proteomes. As expected, Figure S2 of the Supporting Information shows that MPO labeling by **E** was H_2O_2-dependent as little labeling of MPO was observed in the absence of H_2O_2 in the absence (lane 1 in Figure S2A of the Supporting Information) and presence of proteomes (lane 1 in Figure S2B–G of the Supporting Information). However, MPO was labeled to a lesser extent with increasing concentrations of the soluble liver proteomes from human (lanes 2 and 3 in Figure S2B–D of the Supporting Information) and mouse (lanes 2 and 3 in Figure S2E–G of the Supporting Information). This is most likely due to the rapid metabolism of H_2O_2 by other enzymes that are present in liver, which then limits the amount of H_2O_2 that is available for a highly H_2O_2-dependent MPO reaction with **E**. This is evidenced by the greater extent of MPO labeling by **E** at 100 versus 30 μM H_2O_2 in the presence of liver proteomes under all conditions (lane 3 vs lane 2 in Figure S2B–G of the Supporting Information). In addition to MPO labeling, other protein targets were labeled by **E** at ~17 and 25 kDa with other lighter bands at ~40 kDa in the human soluble liver proteome. Similarly, a number of proteins at ~17 and 25 kDa were labeled by **E** from the mouse soluble liver proteomes. Interestingly, all of the aforementioned protein labeling by **E** was H_2O_2-dependent as none of these proteins were labeled in the absence of H_2O_2 (lane 1 in Figure S2B–G of the Supporting Information)

To further investigate the results described above in more detail, we next analyzed the protein targets of **E** in the presence or absence of MPO. As shown in Figure 10, when liver proteomes from human (Figure 10B) and mouse (Figure 10D) were treated with **E** in the presence of MPO, both MPO and other protein targets (bands with asterisks in lane 4 in Figure 10B,D) were labeled by **E** in a H_2O_2-dependent manner as little or no labeling of MPO and protein targets was observed in the absence of H_2O_2 (lane 1 in Figure 10B,D). Similar negligible labeling of protein targets was observed when proteomes were first incubated with the parent inhibitor **A** prior to labeling by **E** in the presence (lane 3 in Figure 10B,D) or absence (lane 2 in Figure 10B,D) of H_2O_2, indicating **E** competes for the same site as **A** in both MPO and these proteins. However, in the absence of MPO, **E** did not label any protein targets in liver soluble proteomes from human (Figure 10C) or mouse (Figure 10E) in the presence (lane 4 in Figure 10C,E) or absence of H_2O_2 (lane 1 in Figure 10C,E). Similarly minimal or no labeling of any proteins by **E** was observed when the proteomes were first incubated with the parent inhibitor **A** prior to labeling by **E** in the presence (lane 3 in Figure 10C,E) or absence of H_2O_2 (lane 2 in Figure 10C,E). To ensure that the preparation of soluble liver proteomes from human and mouse had not caused denaturation or degradation of proteins, each proteome was labeled with the serine hydrolase activity-based probe, fluorophosphonate-TAMRA

dx.doi.org/10.1021/bi401354d | *Biochemistry* 2013, 52, 9187–9201

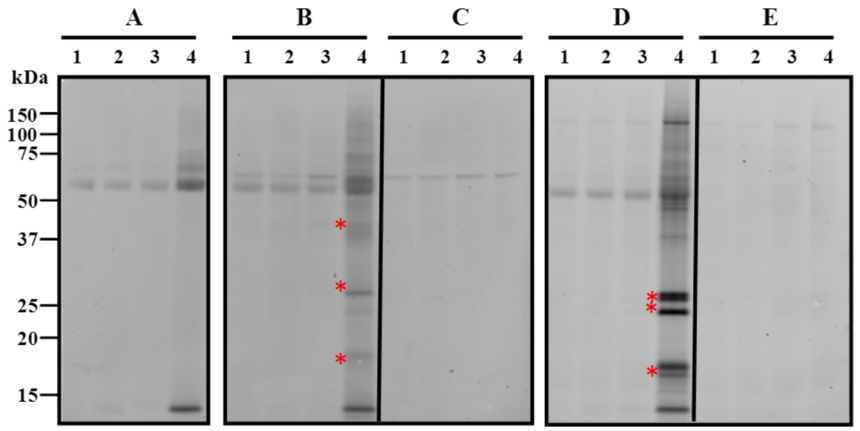

Figure 10. Analysis of protein targets of an alkyne analogue **E** by CC−ABPP. (A) Gel profiles of CC experiments in which MPO was incubated with **E** in the absence (lane 1) or presence of 100 μM H_2O_2 (lane 4) in the absence of proteomes. MPO was pretreated with **A** first before the addition of **E** in the absence (lane 2) or presence of 100 μM H_2O_2 (lane 3). (B and D) Gel profiles of CC−ABPP experiments in which the conditions are the same as in panel A, except that MPO was incubated in the presence of 0.1 mg/mL human (B) or mouse (D) soluble liver proteomes. (C and E) Gel profiles of CC−ABPP experiments in which the human (C) or mouse (E) soluble liver proteome was incubated with **E** in the absence (lane 1) or presence of 100 μM H_2O_2 (lane 4) in the absence of MPO. The soluble liver proteome was pretreated with **A** first before the addition of **E** in the absence (lane 2) or presence of 100 μM H_2O_2 (lane 3). After reacting with catalase, the samples were treated with a rhodamine-azide tag under CC conditions and analyzed by in-gel fluorescence scanning.

(FP-TAMRA). As shown in Figure S3 of the Supporting Information, serine hydrolases were efficiently labeled by FP-TAMRA, indicating that these proteomes contain active enzymes.

Taken together, our data indicate that **A** is unreactive toward soluble liver proteomes from human and mouse. However, in the presence of MPO, **A** labels several protein targets from the same liver proteomes in a H_2O_2-dependent manner.

Compound A Inhibits the MPO-Mediated Modification of ApoA1. 2-Thioxanthines have been reported to inhibit both chlorination and peroxidation activities of MPO.[14] Next we evaluated whether **A** inhibits the chlorinating activity of MPO in a more native system. Chlorination of ApoA1 by the MPO reaction product HOCl has been shown to result in a loss of cholesterol acceptor activity and to alter the electrophoretic mobility of ApoA1 due to fragmentation and dimerization of the protein.[28] For this purpose, we evaluated whether **A** inhibits the chlorination activity by monitoring the MPO-mediated modification of ApoA1 in the presence of **A**. MPO was incubated with ApoA1 in the presence of H_2O_2 and NaCl for 2 h, and the reaction was subjected to SDS−PAGE and Western blot analysis using an anti-ApoA1 antibody. As shown in Figure 11, increased heterogeneity, including fragmentation and dimerization of the recombinant ApoA1, was observed in the complete MPO/H_2O_2/Cl^- system (lane 1 vs lane 3), presumably because of the chlorination activity (HOCl production) of MPO. In contrast, control reactions in the absence of MPO yielded no ApoA1 modification (lane 4). All of the MPO-mediated effects on ApoA1 were inhibited to a near completion by 30 μM **A** (lane 2). These results illustrate that **A** inhibits the chlorination activity of MPO in a native ApoA1 system.

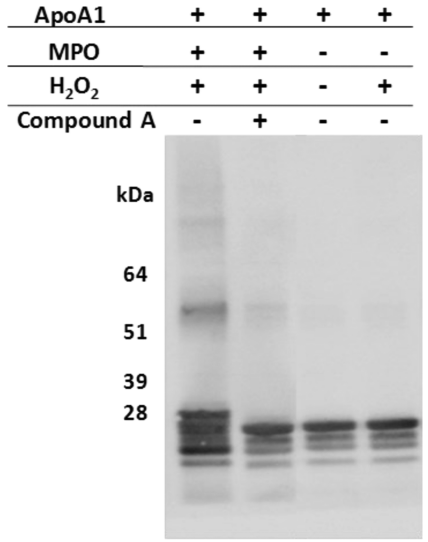

Figure 11. Compound **A** inhibits the MPO-mediated modification of ApoA1. The MPO reactions were conducted with 57 nM MPO, 5 μM ApoA1, and 35.5 μM H_2O_2 in the presence or absence of 30 μM **A** for 2 h under the conditions described in Materials and Methods. Reaction mixtures were subjected to SDS−PAGE and Western blot analysis using an ApoA1 specific antibody. Increased levels of fragmentation and dimerization of ApoA1 are observed for reaction mixtures with MPO and H_2O_2 (lane 1 vs lane 3), which was inhibited to a near completion by 30 μM **A** (lane 2). No fragmentation or dimerization was observed in the absence of MPO (lane 4).

DISCUSSION

Myeloperoxidase is a heme-containing enzyme stored in neutrophils that utilizes H_2O_2 to generate HOCl and other oxidants used in combating bacteria and pathogens. However, excess MPO activity has been implicated in many diseases such as atherosclerosis, cardiac dysfunction, Parkinson's disease, and rheumatoid arthritis.[3−7]

Despite the high level of interest in MPO as a therapeutic target, there have been limited reports about the characterization of MPO inhibitors that allow for studying and evaluating the effects of pharmacological inhibition of MPO. Almost all known MPO inhibitors, including hydroxamic acids, indoles, and tryptamines, inhibit the chlorination activity of MPO by acting as peroxidase substrates and diverting the enzyme from the chlorination cycle to the peroxidation cycle.[29−31] Many of these compounds promote the formation of compound II by being readily oxidized by compound I, one of the strongest oxidizing

dx.doi.org/10.1021/bi401354d | *Biochemistry* 2013, 52, 9187−9201

enzyme intermediates found *in vivo*, but they do not then react with compound II and prevent the enzyme from completing the reaction cycle. However, accumulated compound II can be easily reduced back to the native enzyme form by many other electron donors such as urate,[32] ascorbate,[33] tyrosine,[34] or superoxide anion[35,36] found *in vivo*. Thus, the mode of inhibition by these inhibitors is reversible, and the *in vivo* inhibitory effect of these reagents is rather ineffective.[1]

Recently, 2-thioxanthines were reported to be mechanism-based inactivators of MPO.[14] However, designating compounds as mechanism-based inactivators requires that they display all the distinguishing features of mechanism-based inactivators.[18,37] Therefore, we conducted detailed mechanistic studies for the 2-thioxanthine derivatives. It was critical that we utilized a continuous MPO assay for detailed mechanistic characterization of MPO inhibitors as this assay allows kinetic evaluation of inhibitors and determination of potency as the second-order rate constant k_{inact}/K_I ratios. This k_{inact}/K_I ratio has been described as the best measure of potency for covalent, irreversible inhibitors.[18] Unlike IC_{50} values, k_{inact}/K_I ratios do not vary with incubation time or enzyme concentration in the assay and therefore are critical for developing structure−activity relationships for irreversible inhibitors.

We have described herein that the inhibition of MPO by **A** displays all the required features of a mechanism-based inactivator. Initial kinetic studies revealed time-dependent inhibition in the reaction progress curves (Figure 3A) with saturable inactivation kinetics consistent with a two-step mechanism for MPO inactivation (Figure 3B) and an inhibition potency (k_{inact}/K_I ratio) of 8470 ± 780 M^{-1} s^{-1}. Inhibition of MPO by **A** critically depends on the presence of the sulfur atom because **B**, in which the sulfur atom in **A** is replaced with oxygen, was completely inactive. Rapid dilution experiments with H_2O_2 in the preincubation (Figure 4) confirmed that **A** is acting via a covalent, irreversible mechanism. Using a rapid dilution experiment without H_2O_2 in the preincubation (Figure 4) and spectral scan analysis (Figure 5), we confirmed that MPO catalysis is involved in inhibition by **A**, an important feature of a mechanism-based inactivator. We illustrated that **A** is competitive with the Amplex Red substrate (Figure 6), and studies showing no effect of the trapping agents DMPO and GSH (to scavenge any radical species that are produced during the catalytic cycle) on MPO inhibition by **A** were provided as further evidence that covalent modification occurs prior to release of the activated inhibitory species.

Scheme 1 summarizes the proposed mechanism for inactivation of MPO by **A** from this study. **A** initially binds to MPO compound I, which is generated from native MPO and H_2O_2. **A** is oxidized by MPO compound I, which generates compound II with a second-order rate constant k_3 of (0.801 ± 0.05) × 10^6 M^{-1} s^{-1} and an activated inhibitory species of **A**. This activated species can then inhibit MPO by covalently modifying the heme moiety or dissociate from the enzyme and is released into solution. The resulting covalent modification of the MPO heme "locks" MPO in an inactivated form, which cannot be converted to the native form. This mechanism is in contrast to that of most reversible MPO inhibitors described above;[29−31] although they are oxidized by compound I yielding compound II, the latter is readily reduced back to the native form of MPO by many other electron donors *in vivo*.

There are other reports of mechanism-based inhibitors of MPO. For example, an anti-thyroid drug propylthiouracil (PTU), an inhibitor of thyroid peroxidase, has been shown to also act as a peroxidase substrate that covalently binds to MPO;[38] however, detailed data providing evidence of mechanism-based inactivation or the exact location of covalent modification have not been reported. ABAH has also been reported to be a mechanism-based inactivator of MPO and is oxidized by compound I and compound II. The resulting radicals were shown to mediate the reduction of native ferric MPO to ferrous MPO, which is readily converted into its dioxyggen complex [compound III (reactions V and VI)].[26,27] On the basis of our detailed spectral scan analysis of MPO with **A**, there is no evidence of compound III formation, which is in contrast to ABAH. **A** inhibits MPO by reducing compound I to compound II with a second-order rate constant k_3 of (0.801 ± 0.056) × 10^6 M^{-1} s^{-1} (Scheme 1) without compound III formation.

One of several potential clinical advantages of mechanism-based inactivators is target specificity because formation of the inactivating species is intimately associated with the unique catalytic function of the enzyme active site.[18] We assessed the *in vitro* selectivity of **A** against a broad panel of more than 100 targets, including receptors, enzymes, transporters, and ion channels (Table S1 of the Supporting Information). The results listed in Table S2 of the Supporting Information illustrate that **A** is selective, because **A** at 10 μM does not inhibit any targets assessed to a significant extent.

Importantly, we also assessed the selectivity of **A** in proteomes to determine whether **A** can form covalent adducts with any proteins in soluble liver proteomes derived from human and mouse sources. The relatively high partition ratio of 15.6 we determined for **A** indicates that a covalent MPO−**A** adduct is formed inefficiently, occurring only once for every 16.6 catalytic cycles. To assess the selectivity of **A** against proteomes, we synthesized **E**, an alkyne analogue of **A**, which maintained a high potency for MPO inhibition as well as a partition ratio similar to that of the parent inhibitor **A** (Figure 7 and Figure S1 of the Supporting Information). We directly analyzed protein targets of **E** by CC−ABPP in human and mouse soluble liver proteomes. In the absence of MPO, **E** was found to be unreactive in labeling soluble liver proteomes from human and mouse. However, **E** covalently modified multiple other protein targets in the presence of MPO, presumably because of the release of activated **E** products from the MPO-mediated reaction. Further work is warranted to assess whether the activated species of **E** would label other proteins using more biologically relevant proteomes in which MPO is endogenously expressed or when MPO is inhibited *in vivo*. These studies should reveal the extent of modifications of other proteins as well as the distance the MPO-activated species of **E** can diffuse away from the MPO binding site. It would also be of interest to identify those protein targets modified by **E**.

Our extensive mechanistic and pharmacological analysis combined with selectivity assessment of **A** utilizing CC−ABPP demonstrates that **A** has the potential to serve as a useful pharmacological tool for studying and evaluating pharmacological inhibition of MPO. However, this study also highlights the fact that **A** can covalently modify off-target proteins in the presence of MPO.

We propose the utilization of an alkyne analogue followed by CC as a general method for assessing the covalent modification of heme-containing enzymes by a potential heme-modifying inhibitor. Methods involved in this process are often difficult as they require a synthesis of radioactive inhibitors or a purification of the heme-containing fragments by protease digestion followed by extensive multistage MS analysis. This procedure is lengthy

dx.doi.org/10.1021/bi401354d | *Biochemistry* 2013, 52, 9187−9201

and often requires harsh conditions, including high temperatures and low and high pH values, which could result in the loss of inhibitor adducts. Furthermore, utilization of an alkyne analogue with CC−ABPP offers an opportunity to enrich and identify proteins that are labeled by mechanism-based inhibitors. To the best of our knowledge, this paper describes the first application of CC−ABPP to study inhibitors for the heme peroxidase family of enzymes. This paper also highlights critical methods that could be utilized to guide the discovery and development of next-generation MPO inhibitors.

■ ASSOCIATED CONTENT

Supporting Information

Data showing the selectivity of **A** against a broad panel of 100 targets, determination of the partition ratio for **E**, MPO labeling in the presence of proteomes by an alkyne analogue **E** after CC, and gel images of human and mouse soluble liver proteomes labeled with FP-TAMRA. This material is available free of charge via the Internet at http://pubs.acs.org.

■ AUTHOR INFORMATION

Corresponding Author

*Cardiovascular and Metabolic Diseases Research Unit, Pfizer Worldwide Research and Development, Cambridge, MA 02139. E-mail: kay.ahn@pfizer.com. Phone: (617) 551-3085.

Notes

The authors declare no competing financial interest.

■ ACKNOWLEDGMENTS

We thank James Landro and Ingrid Stock for their initial assessment of the Amplex Red assay for MPO.

■ ABBREVIATIONS

ABAH, 4-aminobenzoic acid hydrazide; ABPP, activity-based protein profiling; ApoA1, apolipoprotein A1; CC, click chemistry; DMPO, 5,5-dimethyl-1-pyrroline *N*-oxide; DMSO, dimethyl sulfoxide; DTPA, diethylenetriaminepentaacetic acid; GSH, reduced glutathione; MPO, myeloperoxidase; RFU, relative fluorescence units; SD, standard deviation.

■ REFERENCES

(1) Malle, E., Furtmuller, P. G., Sattler, W., and Obinger, C. (2007) Myeloperoxidase: A target for new drug development? *Br. J. Pharmacol. 152*, 838−854.

(2) Klebanoff, S. J., Kettle, A. J., Rosen, H., Winterbourn, C. C., and Nauseef, W. M. (2013) Myeloperoxidase: A front-line defender against phagocytosed microorganisms. *J. Leukocyte Biol. 93*, 185−198.

(3) Choi, D. K., Pennathur, S., Perier, C., Tieu, K., Teismann, P., Wu, D. C., Jackson-Lewis, V., Vila, M., Vonsattel, J. P., Heinecke, J. W., and Przedborski, S. (2005) Ablation of the inflammatory enzyme myeloperoxidase mitigates features of Parkinson's disease in mice. *J. Neurosci. 25*, 6594−6600.

(4) Nicholls, S. J., and Hazen, S. L. (2009) Myeloperoxidase, modified lipoproteins, and atherogenesis. *J. Lipid Res. 50* (Suppl.), S346−S351.

(5) Nicholls, S. J., Zheng, L., and Hazen, S. L. (2005) Formation of dysfunctional high-density lipoprotein by myeloperoxidase. *Trends Cardiovasc. Med. 15*, 212−219.

(6) Rudolph, V., Andrie, R. P., Rudolph, T. K., Friedrichs, K., Klinke, A., Hirsch-Hoffmann, B., Schwoerer, A. P., Lau, D., Fu, X., Klingel, K., Sydow, K., Didie, M., Seniuk, A., von Leitner, E. C., Szoecs, K., Schrickel, J. W., Treede, H., Wenzel, U., Lewalter, T., Nickenig, G., Zimmermann, W. H., Meinertz, T., Boger, R. H., Reichenspurner, H., Freeman, B. A., Eschenhagen, T., Ehmke, H., Hazen, S. L., Willems, S., and Baldus, S. (2010) Myeloperoxidase acts as a profibrotic mediator of atrial fibrillation. *Nat. Med. 16*, 470−474.

(7) Stamp, L. K., Khalilova, I., Tarr, J. M., Senthilmohan, R., Turner, R., Haigh, R. C., Winyard, P. G., and Kettle, A. J. (2012) Myeloperoxidase and oxidative stress in rheumatoid arthritis. *Rheumatology (Oxford, U.K.) 51*, 1796−1803.

(8) Fiedler, T. J., Davey, C. A., and Fenna, R. E. (2000) X-ray crystal structure and characterization of halide-binding sites of human myeloperoxidase at 1.8 Å resolution. *J. Biol. Chem. 275*, 11964−11971.

(9) Taylor, K. L., Strobel, F., Yue, K. T., Ram, P., Pohl, J., Woods, A. S., and Kinkade, J. M., Jr. (1995) Isolation and identification of a protoheme IX derivative released during autolytic cleavage of human myeloperoxidase. *Arch. Biochem. Biophys. 316*, 635−642.

(10) Fenna, R., Zeng, J., and Davey, C. (1995) Structure of the green heme in myeloperoxidase. *Arch. Biochem. Biophys. 316*, 653−656.

(11) Zederbauer, M., Furtmuller, P. G., Brogioni, S., Jakopitsch, C., Smulevich, G., and Obinger, C. (2007) Heme to protein linkages in mammalian peroxidases: Impact on spectroscopic, redox and catalytic properties. *Nat. Prod. Rep. 24*, 571−584.

(12) Furtmuller, P. G., Zederbauer, M., Jantschko, W., Helm, J., Bogner, M., Jakopitsch, C., and Obinger, C. (2006) Active site structure and catalytic mechanisms of human peroxidases. *Arch. Biochem. Biophys. 445*, 199−213.

(13) Furtmüller, P. G., Burner, U., and Obinger, C. (1998) Reaction of Myeloperoxidase Compound I with Chloride, Bromide, Iodide, and Thiocyanate. *Biochemistry 37*, 17923−17930.

(14) Tiden, A. K., Sjogren, T., Svensson, M., Bernlind, A., Senthilmohan, R., Auchere, F., Norman, H., Markgren, P. O., Gustavsson, S., Schmidt, S., Lundquist, S., Forbes, L. V., Magon, N. J., Paton, L. N., Jameson, G. N., Eriksson, H., and Kettle, A. J. (2011) 2-Thioxanthines are mechanism-based inactivators of myeloperoxidase that block oxidative stress during inflammation. *J. Biol. Chem. 286*, 37578−37589.

(15) Geoghegan, K. F., Varghese, A. H., Feng, X., Bessire, A. J., Conboy, J. J., Ruggeri, R. B., Ahn, K., Spath, S. N., Filippov, S. V., Conrad, S. J., Carpino, P. A., Guimaraes, C. R., and Vajdos, F. F. (2012) Deconstruction of activity-dependent covalent modification of heme in human neutrophil myeloperoxidase by multistage mass spectrometry (MS^4). *Biochemistry 51*, 2065−2077.

(16) Tiden, A.-K. (2007) Preparation of 2-thioxanthines as myeloperoxidase (MPO) inhibitors. WO 2007142576.

(17) Gomes, A., Fernandes, E., and Lima, J. L. (2005) Fluorescence probes used for detection of reactive oxygen species. *J. Biochem. Biophys. Methods 65*, 45−80.

(18) Copeland, R. A. (2005) *Evaluation of Enzyme Inhibitors in Drug Discovery: A Guide for Medicinal Chemists and Pharmacologists*, Wiley, Hoboken, NJ.

(19) Ahn, K., Johnson, D. S., Mileni, M., Beidler, D., Long, J. Z., McKinney, M. K., Weerapana, E., Sadagopan, N., Liimatta, M., Smith, S. E., Lazerwith, S., Stiff, C., Kamtekar, S., Bhattacharya, K., Zhang, Y., Swaney, S., Van Becelaere, K., Stevens, R. C., and Cravatt, B. F. (2009) Discovery and characterization of a highly selective FAAH inhibitor that reduces inflammatory pain. *Chem. Biol. 16*, 411−420.

(20) Speers, A. E., and Cravatt, B. F. (2004) Profiling enzyme activities in vivo using click chemistry methods. *Chem. Biol. 11*, 535−546.

(21) Agner, K. (1963) Studies on Myeloperoxidase Activity Spectrophotometry of the MPO-H_2O_2 compound. *Acta Chem. Scand. 17*, S332−S338.

(22) Andrews, P. C., and Krinsky, N. I. (1982) A kinetic analysis of the interaction of human myeloperoxidase with hydrogen peroxide, chloride ions, and protons. *J. Biol. Chem. 257*, 13240−13245.

(23) Paumann-Page, M., Furtmuller, P. G., Hofbauer, S., Paton, L. N., Obinger, C., and Kettle, A. J. (2013) Inactivation of human myeloperoxidase by hydrogen peroxide. *Arch. Biochem. Biophys. 539*, 51−62.

(24) Hoogland, H., van Kuilenburg, A., van Riel, C., Muijsers, A. O., and Wever, R. (1987) Spectral properties of myeloperoxidase compounds II and III. *Biochim. Biophys. Acta 916*, 76−82.

(25) Marquez, L. A., Huang, J. T., and Dunford, H. B. (1994) Spectral and kinetic studies on the formation of myeloperoxidase compounds I and II: Roles of hydrogen peroxide and superoxide. *Biochemistry 33*, 1447−1454.
(26) Kettle, A. J., Gedye, C. A., and Winterbourn, C. C. (1997) Mechanism of inactivation of myeloperoxidase by 4-aminobenzoic acid hydrazide. *Biochem. J. 321*, 503−508.
(27) Burner, U., Obinger, C., Paumann, M., Furtmuller, P. G., and Kettle, A. J. (1999) Transient and steady-state kinetics of the oxidation of substituted benzoic acid hydrazides by myeloperoxidase. *J. Biol. Chem. 274*, 9494−9502.
(28) Peng, D. Q., Wu, Z., Brubaker, G., Zheng, L., Settle, M., Gross, E., Kinter, M., Hazen, S. L., and Smith, J. D. (2005) Tyrosine modification is not required for myeloperoxidase-induced loss of apolipoprotein A-I functional activities. *J. Biol. Chem. 280*, 33775−33784.
(29) Ikeda-Saito, M., Shelley, D. A., Lu, L., Booth, K. S., Caughey, W. S., and Kimura, S. (1991) Salicylhydroxamic acid inhibits myeloperoxidase activity. *J. Biol. Chem. 266*, 3611−3616.
(30) Jantschko, W., Furtmuller, P. G., Zederbauer, M., Neugschwandtner, K., Lehner, I., Jakopitsch, C., Arnhold, J., and Obinger, C. (2005) Exploitation of the unusual thermodynamic properties of human myeloperoxidase in inhibitor design. *Biochem. Pharmacol. 69*, 1149−1157.
(31) Davies, B., and Edwards, S. W. (1989) Inhibition of myeloperoxidase by salicylhydroxamic acid. *Biochem. J. 258*, 801−806.
(32) Meotti, F. C., Jameson, G. N., Turner, R., Harwood, D. T., Stockwell, S., Rees, M. D., Thomas, S. R., and Kettle, A. J. (2011) Urate as a physiological substrate for myeloperoxidase: Implications for hyperuricemia and inflammation. *J. Biol. Chem. 286*, 12901−12911.
(33) Hsuanyu, Y., and Dunford, H. B. (1999) Oxidation of clozapine and ascorbate by myeloperoxidase. *Arch. Biochem. Biophys. 368*, 413−420.
(34) Marquez, L. A., and Dunford, H. B. (1995) Kinetics of oxidation of tyrosine and dityrosine by myeloperoxidase compounds I and II. Implications for lipoprotein peroxidation studies. *J. Biol. Chem. 270*, 30434−30440.
(35) Kettle, A. J., Gedye, C. A., and Winterbourn, C. C. (1993) Superoxide is an antagonist of antiinflammatory drugs that inhibit hypochlorous acid production by myeloperoxidase. *Biochem. Pharmacol. 45*, 2003−2010.
(36) Kettle, A. J., Maroz, A., Woodroffe, G., Winterbourn, C. C., and Anderson, R. F. (2011) Spectral and kinetic evidence for reaction of superoxide with compound I of myeloperoxidase. *Free Radical Biol. Med. 51*, 2190−2194.
(37) Silverman, R. B. (1995) Mechanism-based enzyme inactivators. *Methods Enzymol. 249*, 240−283.
(38) Lee, E., Miki, Y., Katsura, H., and Kariya, K. (1990) Mechanism of inactivation of myeloperoxidase by propylthiouracil. *Biochem. Pharmacol. 39*, 1467−1471.